Optical properties, morphology and elemental composition of atmospheric particles at T1 supersite on MILAGRO campaign

G. Carabali[1], R. Mamani-Paco[1], T. Castro[1], O. Peralta[1], E. Herrera[2], and B. Trujillo[2]

[1] Centro de Ciencias de la Atmósfera, UNAM, México

[2] Centro de Investigaciones de Materiales Avanzados, Chihuahua, México

Correspondence to: T. Castro (telma@atmosfera.unam.mx)

Abstract

Atmospheric particles were sampled at T1 supersite (19°43' N latitude, 98°58' W longitude, and 2340 meters above sea level) during MILAGRO campaign, on March 2006. T1 was located at the north of Mexico City Metropolitan Area (MCMA). Aerosol sampling was done by placing transmission electron microscope (TEM) copper grids on the last 5 of an 8-stage MOUDI cascade impactor (d_{50} = 1.8, 1.0, 0.56, 0.32, and 0.18 µm). Samples were obtained at 6:00 – 9:00, 11:00 – 14:00, 16:00 – 19:00, and 21:00 – 24:00 periods, local time. Absorption and scattering coefficients, and particles concentration (0.01 – 3 µm aerodynamic diameter) were measured simultaneously using a PSAP absorption photometer (operated at 550 nm), a portable integrating nephelometer (at 530 nm) and a CPC particle counter. Particle images were acquired at different magnifications using a CM 200 Phillips TEM-EDAX system. Also, energy dispersive X-ray spectroscopy (EDS) was used to determine the elemental composition of particles. The morphology of atmospheric particles for two aerodynamic diameters (0.18 and 1.8 µm) was compared using border-based fractal dimension.

Particles sampled under Mexico City pollution influence showed not much variability, suggesting that more compact particles are present in larger sizes (d_{50} = 1.8 µm), which may be attributed to aerosol aging and secondary aerosol formation. Between 06:00 and 09:00, smaller particles (d_{50} = 0.18 µm) had more irregular shapes resulting in a higher average fractal dimension for samples with more local influence. EDS analysis in d_{50} = 0.18 µm particles showed high contents of carbonaceous material, Si, Fe, K, and Co. Perhaps it indicates an impact from industrial and vehicles emissions on atmospheric particles at T1.

1 Introduction

Most megacities in the developing world lie in subtropical and tropical latitudes, with a population growth so intensive that urban areas are constantly increasing without adequate planning. Mexico City is one of those, it is located at 2240 masl (meters above sea level), and has high solar irradiance, light winds and heterogeneous atmospheric removal processes (Raga et al*,* 2001) that are quite different from other megacities at midlatitudes. This situation is moreover complicated by the plumes from the Popocatepetl volcano, a natural source of gases and sulfate enriched aerosols. During volcanic activity the plumes contain significant quantities of aerosols composed by sulfates, especially in the smaller sizes (Jiménez et al, 2004).

In Mexico City, the light absorbed by atmospheric aerosols is mainly due to particles from motor vehicles exhausts, especially diesel engines (Molina and Molina, 2002). In the mornings there are fresh particle emissions with high black carbon (BC) contents, and along the day they get coated by secondary organics (Salcedo et al, 2006; Paredes-Miranda et al, 2009) contributing to decrease the particle single scattering albedo. BC absorbs solar radiation and can be present in external and internal mixtures, or even create a BC core in the particle that may be enclosed in a well-mixed shell, thus atmospheric particles optical properties change according to the internal distribution of chemical species. For example, the absorption coefficient of non-absorbent particles with mixed BC is larger for an internal mixture than for an external one (Horvath et al, 1997).

As particles age, inorganic (i.e. nitrates and sulfates) and organic species coat them. Also, it seems that water influences the amount of sulfates present in particles, so in days with high relative humidity a larger fraction of sulfates has been reported (Baumgardner et al, 2000).

Many studies on morphology and chemical composition observed by electron microscopy (Dye et al, 2000; Xiong and Friedlander, 2001; Katrinak et al, 1993; Okada and Heintzenberg, 2003) report different shapes of atmospheric particles (spheres, aggregates, and irregularly shaped).

Some studies classify particles based on a basic elemental composition and on morphology. Some authors (Mogo et al, 2005; Li and Shao, 2009) grouped atmospheric particles into the following groups: mineral, Ca-S, S-rich, K-rich, organic, soot, fly ash, and metal.

In this research we used a MOUDI impactor to sample atmospheric particles at T1 supersite during MILAGRO campaign on March 2006 (Molina et al, 2010) and observed the morphology of individual particles with a transmission electronic microscope (TEM), and then calculated their border-based fractal dimensions (D_f). Also, energy dispersive X-ray spectroscopy (EDS) was used to get information about the elemental chemical composition for some of them. We compared two sampling days, one of them with not a clear influence (Wednesday, March 15, 2006) from the pollution plume from Mexico City, and the other one directly influenced by city emissions (Sunday, March 19, 2006).

We only focused on d_{50} = 1.8 and d_{50} = 0.18 μm aerodynamic diameters particles. The fractal dimension for particles wrapped in those sizes tends to be more sensitive to changes in ambient weather conditions (Mamani-Paco, 2004).

2 Experimental method

2.1 Aerosol particles sampling

T1 was located at the Universidad Tecnológica de Tecámac, State of Mexico, with coordinates 19°43' N latitude and 98°58' W longitude; it is at 2340 meters above sea level. The site was towards the north of Mexico City Metropolitan Area (MCMA), and represented a place where emissions are fresh and well mixed (Molina et al, 2010).

From 1 to 31 March 2006, we placed a particle soot / absorption photometer (PSAP), operated at λ = 565 nm, and a nephelometer model M903, operated at λ = 530 nm, (both from Radiance Research, Inc.) to measure particles optical properties. Both instruments were connected to a particle counter (CPC) model 3010 (TSI, Inc.), which measures particles concentrations within 0.01 - 3 μm diameter range. The sampling system was 4 m above the ground level.

Also, we used two eight-stage micro orifice uniform deposit impactors (MOUDI) model MSP 100 to collect atmospheric particles with different aerodynamic diameters every two days. On the last 5 MOUDI stages (d_{50} = 1.8 μm, 1.0 μm, 0.56 μm, 0.32 μm, and 0.18 μm) we placed transmission electron microscope grids (LF-200-Cu mesh grids) coated with collodion.

Particle sampling schedules were established for early morning (6:00 - 9:00), noon (11:00 - 14:00), afternoon (16:00 - 19:00), and evening (21:00 - 24:00) local time. Also, meso meteorological model MM5 predictions (de Foy et al, 2006) and meteorological data at T1 indicated the wind direction prevailing from Mexico City, hence we classified the days with and without a clear influence of pollutants to sample particles with the impactors.

2.2 TEM microscopy and elemental chemical analysis of atmospheric particles

The morphology and elemental chemical composition of atmospheric particles were obtained using a CM 200 Phillips TEM-EDAX system. TEM provided high resolution images for particles and EDS information about their elemental composition.

Images were analyzed and fractal dimensions were calculated for at least 30 individual particles per sample, based on their perimeter (Kindratenko et al, 1994). Fractal parameters for 500 particles were calculated. Samples were taken every other day from March 1 to March 30 (at T1). With perimeter fractal dimensions sorted by sizes and sampling times, morphology and aerosol aging were studied. Dye et al (2000) and Kindratenko et al (1994) have observed aerosol physical changes with similar procedures.

2.3 Fractal dimension calculation

Particle digital images were processed using Scion Image software (http://www.scioncorp.com/) for image optimization and extraction of (x,y) particle coordinates analysis. The program additionally provides the particle's area and perimeter length in pixels. The particle border-based (perimeter) fractal dimension is then calculated by a FORTRAN code developed at the University of Connecticut (Newman, 2001; Mamani-Paco, 2004). The code used the definition of border-based fractal dimension, defined by the following equation (Kaye, 1994; Mandelbrot, 1967):

$$L(\lambda) = k\lambda^{1-D_f}$$

where L is the particle perimeter, λ is the particle's boundary step size (the length by which the perimeter is cut in smaller pieces), k is a positive constant factor, and D_f is the fractal dimension. A Richardson plot was used to obtain the slope and the corresponding fractal dimensions (Kaye, 1994).

3 Results

3.1 Meteorological conditions

The meso meteorological model, version 5, MM5 (de Foy et al, 2006) and the meteorological data recorded at T1 supersite provided information about the days with and without a clear MCMA plume influence. We choose Wednesday, March 15, 2006 and Sunday, March 19, 2006 to compare results, because they are clear days with different meteorological conditions that hamper or promote the pollutants transport emitted at MCMA to the site (Fast et al, 2007). On March 15, wind direction changes very often prevailing northerlies, while on March 19 the wind prevails southerly, where the MCMA is located. It was assumed that southerly winds carried pollutants from the urban area to the site. Also, samples obtained on those days were good for comparison. Figure 1 shows wind direction and speed time series (local time) for both days.

3.2 Optical properties of particles

Figure 2 shows time series for particle concentration, scattering coefficient (σ_{sct}), absorption coefficient (σ_{abs}), and single scattering albedo (SSA) on both days. On Wednesday, March 15, early in the morning (7:00) local sources generated 50,000 particles per cubic centimeter, within 0.01 - 3 μm diameter, and around 10:00 the concentration decreased to 10,000. There were also episodes from 19:00 to 24:00 where the particles concentrations increased and gradually arrived to 40,000 per cubic centimeter. Temporary changes in meteorological conditions could cause a major accumulation of particles from 6:00 to 9:00 and from 21:00 to 24:00. Northerlies cold winds (Figure 1) at T1 decreased temperatures, promoting a suitable condition to reduce the mixed layer height. On Sunday, March 19, particles concentration increased gradually from 9:00 to 13:00, when the plume of pollutants from MCMA arrived to T1. The little increase in particles number concentration on that day may also result from diluted plumes arriving earlier from Mexico City (de Foy et al, 2006). Particles concentration decreased around 22:00, when the pollution activities ceased at Mexico City.

Scattering coefficient on March 15 increased again early in the morning and after 19:00, but decreased during 12:00 to 18:00. However, on March 19 the σ_{scat} felt down to 40 Mm^{-1} at 10:00, when the particles concentration increased. After 13:00, the scattering increased and finally at 19:00 the values remained at 30 Mm^{-1}. The high scattering values from 13:00 to 18:00 perhaps are caused by the presence of mixed and aged aerosols. That day was characterized by the influence of MCMA pollutants plume prevailing southerly winds (Figure 1). At 21:00, both scattering and absorption coefficients decreased because pollution activities are less intensive. Also, these σ_{scat} values suggest that particles might have a complex chemical composition increasing light scattering. Assuming that particles reached T1 transported into the plume of pollutants, perhaps they were composed by sulfate-coated soot and other volatiles compounds, which favored scattering of radiation rather than absorption (Baumgardner et al, 2007).

Episodes with high absorption coefficient values occurred along the mornings (6:00 - 9:00) on both days. Perhaps, they are caused by fresh vehicular emissions. However, March 15 values are higher than those from March 19. σ_{abs} measured on March 15 may indicate an influence of local sources. On March 19, σ_{abs} does not change much, from 12:00 to 24:00, matching with the southerly wind.

Figure 2 also shows the single-scattering albedo (SSA) calculated on both days. From 09:00 to 18:00, SSA values were ranged between 0.74 – 0.81. March 15 was affected by northerly winds (from Golf of Mexico) and that day had a relative clean atmospheric background. Between 06:00 and 09:00, SSA lower values (~ 0.3) are probably caused by local fresh emissions. The minima values maybe are attributed to the presence of elemental carbon (EC) on atmospheric particles. Doran et al (2007 reported similar values measured at T1, using a multi filter rotating shadow band radiometer.

Table 1 shows the total average for all particles absorption (σ_{abs}) and scattering (σ_{sct}) coefficients values obtained at T1, compared against total averages from other measurements done in a rural area at Pico de Orizaba two years earlier (Márquez et al, 2005) and Mexico City (T0) during the MILAGRO campaign (Marley et al, 2009). The total average σ_{abs} value obtained at T1 is

higher than that reported at Pico de Orizaba in 2005 and lower than T0, meaning that particles are probably a mix from local and remote sources at T1. The total average σ_{sct} value at T1 is between that measured at Pico de Orizaba and T0, because T1 is a semi-rural area influenced by local and remote particle sources. Márquez et al (2005) report σ_{abs} = 17 Mm^{-1} and σ_{scat} = 39 Mm^{-1} average values at Pico de Orizaba and suggest that Popocatépetl volcano fumes and urban settlements affect optical properties of particles.

3.3 Particle morphology

Once meteorological conditions and particle optical characteristics were analyzed for March 15 and 19, the morphology of small (d_{50} = 0.18 µm) and relatively larger (d_{50} = 1.8 µm) fine particles was determined to be used as an additional tool to distinguish freshly emitted and aged fine particles. We were especially interested in soot particles. Figure 3 shows particles TEM images for different sizes sampled at T1. Irregular shape particles were more common in smaller than in large sizes. Figure 4 shows small particles (d_{50} = 0.18 µm) collected at different sampling times; the arrow points to their main structure, which is composed of tiny spherules forming aggregates in most cases. This is a typical structure present in carbonaceous material originated in combustion processes. Complex morphology of particles can be noticed and soot chains are seen attached to round particles resulting in external mixtures. Soot particles were also attached to other more compact units suggesting they were the result of possible aging processes.

Figure 5 presents fractal dimension histograms for small size particles (d_{50} = 0.18 µm) at different sampling times on March 15 and 19. Table 2 presents the basic statistics for this particle size. Average D_f for particles sampled on March 15 between 6:00 and 9:00 was 1.15 ± 0.08, while average D_f for particles sampled on March 19 at the same time was 1.10 ± 0.06. The results for average D_f for the corresponding dates and sampling times (11:00 and 14:00) were 1.09 ± 0.06 and 1.08 ± 0.06, respectively. There is a clear difference on frequency histograms between March 15 and 19 for the 6:00 to 9:00 sampling periods. It could be explained by the presence of freshly emitted aerosols on March 15 and more aged aerosols on March 19. Soot and metal aggregates

can be emitted from local sources such as vehicle emissions and smelters. On March 15, early in the morning (7:00) local sources generated 50,000 particles per cubic centimeter within 0.01 - 3 µm diameter, and around 10:00 the concentration decreased to 10,000 (Figure 2). In Figure 5 histograms for 16:00 - 19:00 and 21:00 - 24:00 sampling periods have similar distribution patterns in both days. In 16:00-19:00 sampling time, particles tend to be more spherical indicating that maybe they are transported from Mexico City to T1. In 21:00 - 24:00, both distributions broadened to include more irregular shapes (higher fractal dimension values). This is likely to be a predominance of particles emitted from local sources.

The morphology of larger size fine particles (d_{50} = 1.8 µm) is reported in Figure 6 at different sampling times for both days. The morphology of larger size particles was expected to be less irregular tending to spherical due to their typical emissions (mechanical processes, chemical processes, aging, and combustion). So, the border-based fractal dimension (D_f) would tend to 1. The average border-based (perimeter) fractal dimensions reported in Table 3 ranged from 1.10 to 1.05. These results agree with what was expected for particles in this size range. The histograms on Figure 6 for 16:00 – 19:00 and 21:00 – 24:00 both days have similar patterns that cannot be distinguished one from another. But in this case, the histograms show a more uniform distribution of fractal dimensions in the period 16:00 to 19:00 and round shapes (D_f tends to 1) in the period 21:00-24:00, probably by aging processes of particles.

In our study, it can be noted that particles with higher aerodynamic diameters tend to have a more spherical shape. Particles with lower aerodynamic diameters reflect the formation of soot with a characteristic irregular (fractal) shape (Kindratenko et al, 1994; Mamani-Paco, 2004). This may indicate different steps in aerosol aging processes; i.e. particles are released to the atmosphere as agglomerates with voids. As they age, by condensation or impaction, voids are filled and the agglomerate morphology becomes more compact.

On March 19, particles concentration increased gradually when the plume of pollutants from MCMA arrived to T1 (9:00 to 13:00), and decreased when the pollution activities ceased at Mexico City (around 22:00).

Also, for March 15, between 06:00 and 09:00 (Figure 5), the frequency histogram indicates a high number of particles with irregular shapes that might be associated with fresh soot emissions (Dye et al, 2000) absorbing radiation efficiently and responsible for the absorption peak that appears early morning on that day (Figure 2). Particle absorption coefficient values for March 15 are higher than those for March 19, and those from March 15 point to an influence of local sources with smaller fine particles having highly irregular morphologies.

3.4 Elemental composition of particles

EDS provides elemental composition with 99% precision detection. Twelve elements were detected on the samples analyzed by EDS. Table 4 presents averaged results on relative elemental composition for particles showed on Figure 3.

Elemental analyses performed on some particles (i.e. Figure 3) demonstrate aggregates with internal mixing. It is evident that small aerodynamic diameter (d_{50} = 0.18 µm) has the highest percentage of C, Fe and Co, in its structure. The last two elements could be released by local sources, such as oxidation in mechanical parts of cars, or metallurgical activities carried out near the area. In Mexico City fresh particulate emissions due to motor vehicle traffic, especially diesel engines are mostly carbonaceous with very low sulfur content (Molina and Molina, 2002), as it is illustrated on Table 4**.** Figure 3 shows particles observed in TEM with several crusted elements, like S, O, Si, Al, Ca, Ti, Mn, Fe, and K.

Particles with d_{50} = 1.8 µm, have low oxygen and carbon percentages, but high K levels (a biomass burning tracer) and other elements, such as Si, Na, Ca, and Al; which are more abundant in clayey soils and rocks (Seinfeld and Pandis, 1998).

4 Conclusions

A previous study by Johnson et al (2005) concluded that MCMA soot particles collected directly from city traffic were mostly irregular and showed physical and chemical differences against soot particles collected in ambient conditions. They also suggested a rapid processing (in the order of hours) of soot by ammonium sulfate leading to internally-mixed particles. The observation applies to particles present under the MCMA plume (Adachi and Buseck, 2008; Moffet et al, 2010). We can then infer that irregular carbonaceous aggregates with high border-based fractal dimensions (D_f close to 2) become more compact in shape (D_f close to 1) as a result of condensation and coagulation processes (aging). Our results for morphology differences between sampling times with and without MCMA plume influence at T1 site agree with these findings. It is important to note that images and morphological information described in this article only correspond to non-volatile components of particulate matter. Our work goes one step further by providing some initial quantification of changes in morphology at a specific aerodynamic diameter (d_{50} = 0.18 µm). Ramsden and Shibaoka (1982); Pósfai et al (2003); Kaegi and Holzer (2003); Li et al (2003) used a similar analysis approach to study aerosol particles properties. In detail quantification of soot particles morphology sampled under different conditions can be employed both in climate and health models.

Elemental composition analysis show different inclusions of inorganic elements grouped (S, K, and Si; Fe, Na, and P) which agree with earlier studies in Mexico City (Johnson et al, 2005). Sulfate inclusions and other components in aged soot particles are probably due to coagulation and collisions processes experienced by aerosols in the atmosphere at the sampling site, which strongly affects their optical properties (Johnson et al, 2005; Marley et al, 2009; García et al, 2010).

Adachi and Buseck (2008) sampled particles on a C130 airplane during MILAGRO campaign and classified them, based on their sampling location (inside or outside MC plume of pollutants) they also used EDS to determine their elemental composition. They found very often S and K in particles ranged between 50 – 2000 nm size, and classified the structures as soot and organic matter. Our analysis shows that S and K contents in d_{50} = 0.18 µm particles represent

respectively around 3.9% and 1%, but it is difficult to compare results between both studies, specially because the C130 samples were taken around 3.1 km above T1 and represent young particles and ours were at the surface characterizing local and transported particles

Moffet at al (2010) analyzed particles sampled at T1 with different X-ray analytical techniques (i.e. microspcopy and absorption) finding at T1 particles homogeneous with spherical shapes and mixed with organic compounds. In our study D_f tends to 1, indicating more spherical shapes. They also found high contents of Al, S, Ca, and Fe in particles sampled at T1, and state that some elements concentrations are due to local emissions. However, the morphology and elemental composition for both sizes (around 0.18 and 1.8 μm) is not conclusive to relate the particles origin with specific human activities in areas nearby T1.

Acknowledgments

The authors would like to thank M. I. Saavedra for helping them in the aerosols optical properties data analysis and gravimetric analysis. We want also to thank L. Molina, J. Gaffney and S. Madronich for the facilities offered during MILAGRO campaign at T1. Also, we want to thank Dulce Nazareth Ramírez for her support on the document edition.

References

Adachi, K. and Buseck, P. R.: Internally mixed soot, sulfates, and organic matter in aerosol particles from Mexico City. Atmos. Chem. Phys., 8, 6469–6481, 2008

Baumgardner, D., Raga, G. B., Kok, G. L., Ogren, J., Rosas, I., Baez, A., and Novakov, T.: On the evolution of aerosol properties at a mountain site above Mexico City, Journal of Geophysical Research, 105, 17, 22243-22253, 2000

Baumgardner, D., Kok, G. L., and Raga, G. B.: On the diurnal variability of particle properties related to light absorbing carbon in Mexico City. Atmos. Chem. Phys., 7, 2517–2526. www.atmos-chem-phys.net/7/2517/2007/, 2007

De Foy, B., Varela, J. R., Molina, L. T., and Molina, M. J.: Rapid ventilation of the Mexico City basin and regional fate of the urban plume. Atmos. Chem. Phys., 6, 2321–2335http://www.atmos-chem-phys.net/6/2321/2006/, 2006

Doran, J. C., Barnard, J. C., Arnott, W. P., Cary, R., Coulter, R., Fast, J. D., Kassianov, E. I., Kleinman, L., Laulaien, N. S., Matin, T., Paredes-Miranda, G., Pekour, M. S., Shaw, W. J., Smith, D. F., Springston, S. R., and Yu, X. Y.: The T1-T2 study: evolution of aerosol properties downwind of Mexico City, Atmos. Chem. Phys., 7, 1585–1598, http://www.atmos-chem-phys.net/7/1585/2007/, 2007

Dye, A. L., Rhead, M. M., and Trier, C. J.: The quantitative morphology of roadside and background urban aerosol in Plymouth, UK. Atmospheric Environment, 34, 3139-3148, 2000

Fast, J. D., de Foy, B. , Acevedo Rosas F., Caetano E., Carmichael, G., Emmons, L., McKenna, D., Mena, M., Skamarock, W., Tie, X., Coulter, R. L., Barnard, J. C., Wiedinmyer, C., and Madronich, S.: A meteorological overview of the MILAGRO field campaigns. Atmos. Chem. Phys., 7, 2233–2257, 2007

García, L. Q., Castro, T., Saavedra, M. I., and Martínez-Arroyo, M. A.: Optical properties of aerosols: southern Mexico City. Atmósfera, 23, 4, 2010

Horvath, H., Catalan, L., and Trier, A.: A study of the aerosol of Santiago de Chile III Light absorbing measurements, Atmospheric Environment, 31, 3737–3744, 1997

Jiménez, J. C., Raga, G. B., Baumgardner, D., Castro, T., Rosas, I., Báez, A.: On the composition of aerosol particles influenced by emissions of the volcano Popocatepetl in Mexico. Natural Hazards, 31: 21-37, 2004

Johnson, K. S., Zuberi, B., Molina, L. T., Molina, M. J., Iedema, M. J., Cowin, J. P., Gaspar, D. J., Wang, C., and Laskin, A.: Processing of soot in an urban environment: Case study from the Mexico City Metropolitan Area. Atmos. Chem. Phys., 5, 3033–3043, 2005

Kaegi, R. and Holzer, L.: Transfer of a single particle for combined ESEM and TEM analyses. Atmospheric Environment, 37, 4353–4359, 2003

Katrinak, K. A., Rez, P., Perkess, P. R., and Buseck, P. R.: Fractal geometry of carbonaceous aggregates from an urban aerosol. Environ. Sci. Technol., 27, 539–547, 1993

Kaye, B. H.: A Random Walk through Fractal Dimensions, 427 pp., 2nd edition, Weinheim; Base1 (Switzerland) ; Cambridge ; New York, NY : VCH, 1994

Kindratenko, V. V., Van Espen, J. M., Treiger, B. A., Van Grieken, R. E.: Fractal dimensional classification of aerosol particles and computer-controlled scanning electron microscopy. Environ. Sci. Technol., 28:2197-2202, 1994

Li, J., Anderson, J. R., and Buseck, P. R.: TEM study of aerosol particles from clean and polluted marine boundary layers over the North Atlantic. J. Geophysical Res., 108, NO. D6, 4189, doi: 10.1029/2002JD002106, 2003

Li, W. and Shao, L.: Transmission electron microscopy study of aerosol particles from the brown hazes in northern China. J. Geophys. Res., 114, D09302, doi: 10.1029/2008JD011285, 2009

Mandelbrot, B. B.: How long is the coastline of Britain? Statistical self similarity and fractional dimension. Science, 156: 636-638, 1967

Mamani-Paco, R.: Morphology distributions and chemical composition of size-selected atmospheric fine particles. PhD dissertation, AAT 3156402, ISBN 0496171003, University of Connecticut, Storrs, CT, 2004

Marley, N. A., Gaffney, J. S., Castro, T., Salcido, A., and Frederick, J.: Measurements of aerosol absorption and scattering in the Mexico City Metropolitan Area during the MILAGRO field

campaign: a comparison of results from the T0 and T1 sites. Atmos. Chem. Phys., 9, 189–206, 2009

Márquez, C., Castro, T., Muhlia, A., Martínez-Arroyo, M. A., and Báez, A.: Measurement of aerosol particles, gases and flux radiation in the National Park Pico de Orizaba, and its relationship to air pollution transport. Atmospheric Environment, 39, 21, 3877-3890, 2005

Molina, L. T. and Molina, M. J.: Air quality in the Mexico Megacity, An integrated assessment, Kluwer Academic, The Netherlands, 408 pp, 2002

Molina, L. T., Madronich, S., Gaffney, J. S., Apel, E., de Foy, B., Fast, J., Ferrare, R., Herndon, S., Jiménez, J. L., Lamb, B., Osornio-Vargas, A. R., Russell, P., Schauer, J. J., Stevens, P. S., Volkamer, R., and Zavala, M.: An overview of the MILAGRO 2006 Campaign: Mexico City emissions and their transport and transformation, Atmos. Chem. Phys., 10, 8697-8760, 2010

Moffet, R. C., Henn, T. R., Tivanski, A. V., Hopkins, R. J., Desyaterik, Y., Kilcoyne, A. L., Tyliszczak, D. T., Fast, J., Barnard, J., Shutthanandan, V., Cliff, S. S., Perry, K. D., Laskin, A., and Gilles, M. K.: Microscopic characterization of carbonaceous aerosol particle aging in the outflow from Mexico City. Atmos. Chem. Phys., 10, 961–976, 2010

Mogo, S., Cachorro, V. E., and De Frutos, A. M.: Morphological, chemical and optical absorbing characterization of aerosols in the urban atmosphere of Valladolid. Atmospheric Chemistry and Physics, 5, 2739-2748, 2005

Newman, M.: Structural characterization of ambient particulate matter using fractal dimensions, University of Connecticut, USA, CHEG 299, 2001

Okada, K. and Heintzenberg, J.: Size distribution, state of mixture, and morphology of urban aerosol particles at given electrical mobilities, Journal of Aerosol Science, 34, 1539–1553, 2003

Paredes-Miranda, G., Arnott, W. P., Jiménez, J. L., Aiken, A. C., Gaffney, J. S., and Marley, N. A.: Primary and secondary contributions to aerosol light scattering and absorption in Mexico City during the MILAGRO 2006 campaign, Atmos. Chem. Phys., 9, 3721-3730, 2009

Pósfai, M., Simonics, R., Li, J., Hobbs, P. V., and Buseck, P. R.: Individual aerosol particles from biomass burning in southern Africa: 1. Composition and distributions of carbonaceous particles. J. Geophys. Res., 108(D13), 8483, doi:10.1029/2002JD002291, 2003

Raga, G., Baumgardner, D., Castro, T., Martínez-Arroyo, M. A., and Navarro-González, R.: Mexico City Air Quality: A Qualitative Review of Gas and Aerosol Measurements (1960-2000). Atmospheric Environment, 35, 4041-4058, 2001

Ramsden, A. R. and Shibaoka, M.: Characterization and analysis of individual fly-ash particles from coal-fired power stations by a combination of optical microscopy, electron microscopy and quantitative electron microprobe analysis, Atmospheric Environment, 16 (9), 2191–2206, 1982

Salcedo, D., Onasch, T. B., Dzepina, K., Canagaratna, M. R., Zhang, Q., Huffman, J. A., De Carlo, P. F., Jayne, J. T., Mortimer, P. Worsnop, D. R., Kolb, C. E., Johnson, K. S., Zuberi, B., Marr, L. C., Volkamer, R., Molina, L. T., Molina, M. J., Cárdenas, B., Bernabé, R. M., Márquez, C., Gaffney, J. S., Marley, N. A., Laskin, A., Shutthanandan, V., Xie, Y., Brune, W., Lesher, R., Shirley, T., and Jiménez, J. L.: Characterization of ambient aerosols in Mexico City during the MCMA-2003 campaign with aerosol mass spectrometry: results from the CENICA Supersite. Atmos. Chem. Phys., 6, 925-946, 2006

Seinfeld, J. H. and Pandis, S. N.: Atmospheric chemistry and physics: from air pollution to climate change, A Wiley-Interscience publication, USA, 1326 pp, 1998

Xiong, C. and Friedlander, S. K.: Morphological properties of atmospheric aerosol aggregates, Proceedings of the National Academy of Sciences USA 98, 11851–11856, available online at: www.pnas.org/cgi/doi/10.1073/pnas.211376098, 2001

Figures and tables

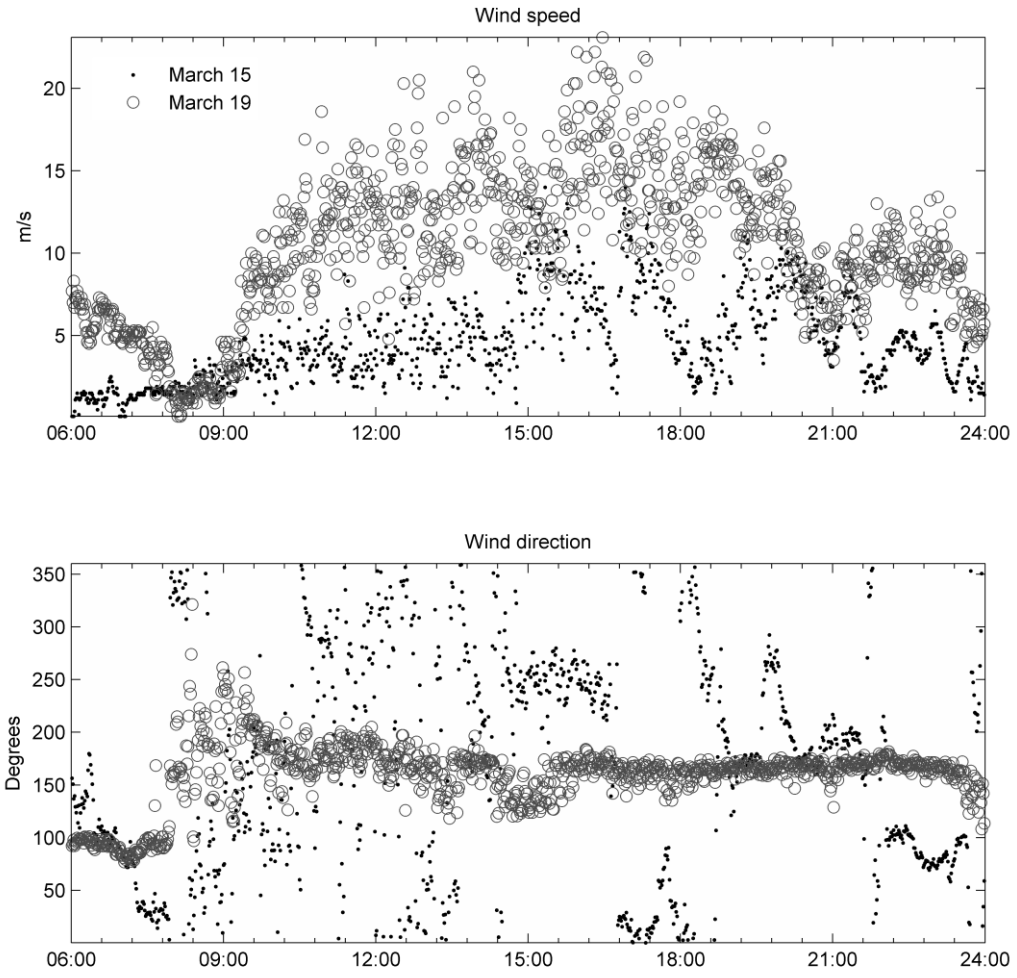

Figure 1 Time series for wind speed and direction at T1 on March 15 and 19

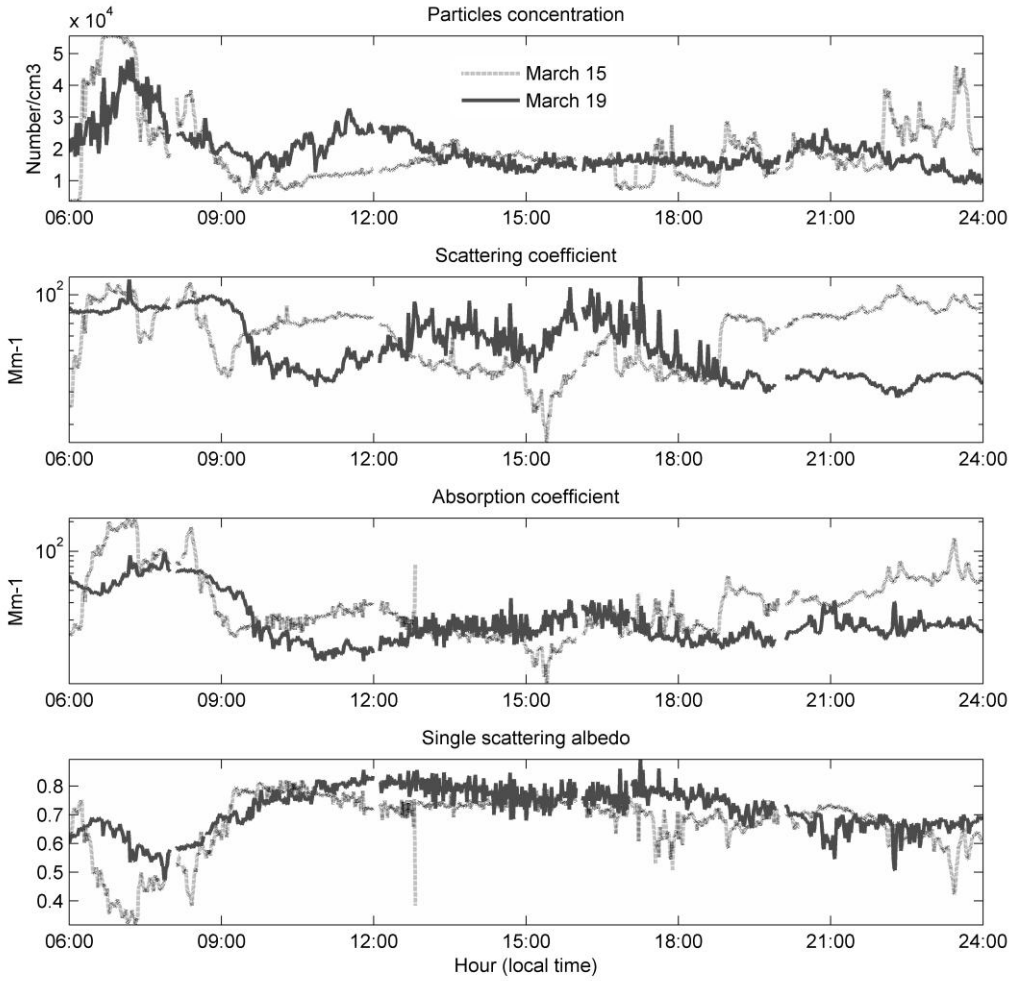

Figure 2 Time series for particles concentration, absorption and scattering coefficients, and single scattering albedo for March 15 and 19

5

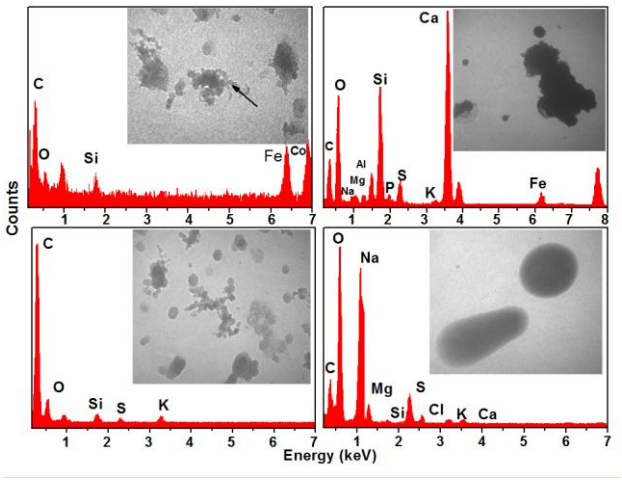

Figure 3 TEM images and elemental analysis of atmospheric particles. Particles sampled on March 15 (row above) and March 19 (row below). Aerodynamic diameter 0.18 μm (left column) and 1.8 μm (right column)

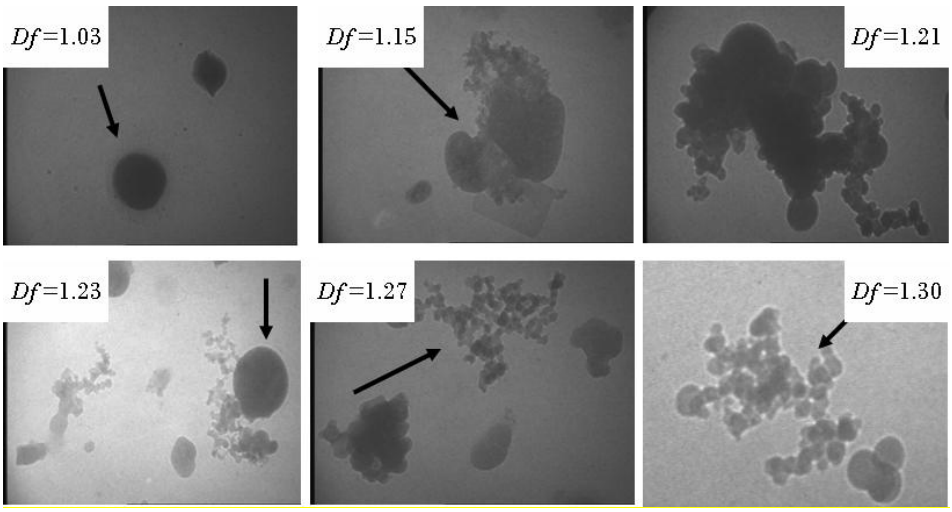

Figure 4 TEM images with different dimension fractal (D_f) values for atmospheric particles with 0.18 μm aerodynamic diameter

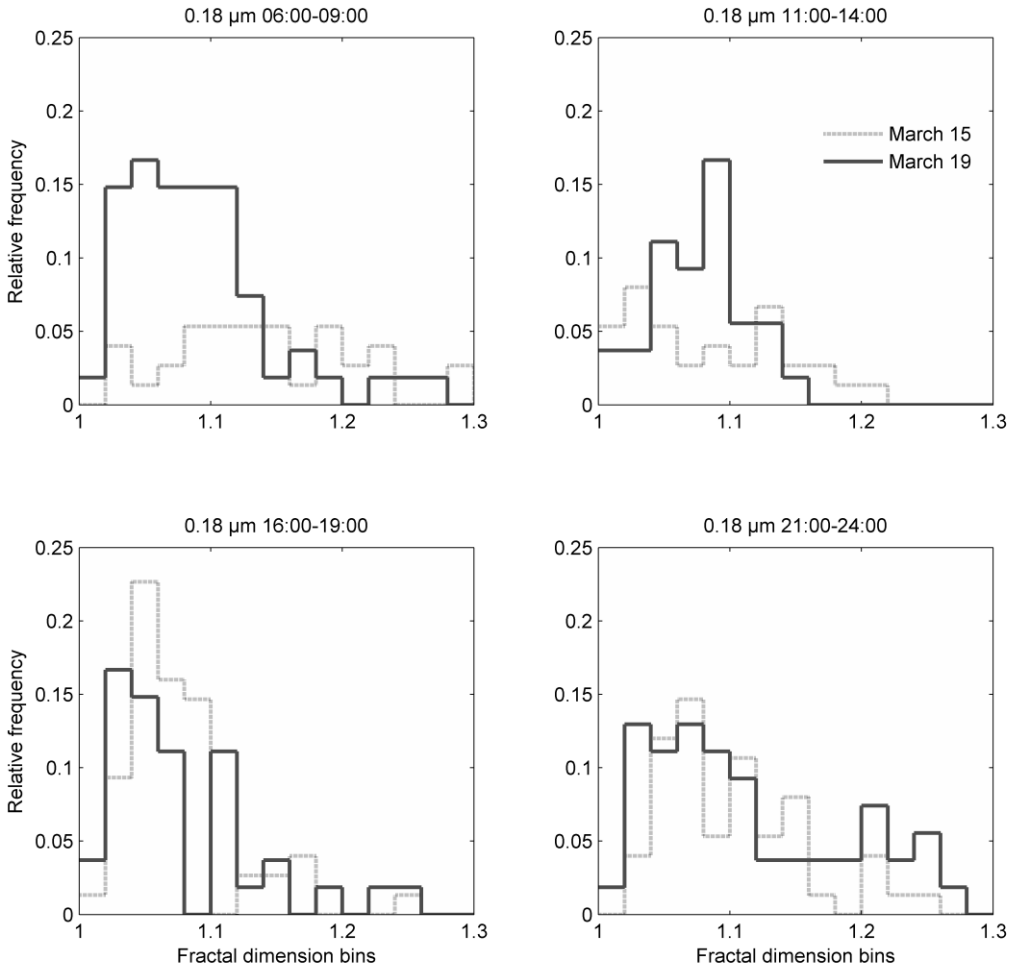

Figure 5 D_f particles histograms (0.18 µm aerodynamic diameter), sorted by sampling time.

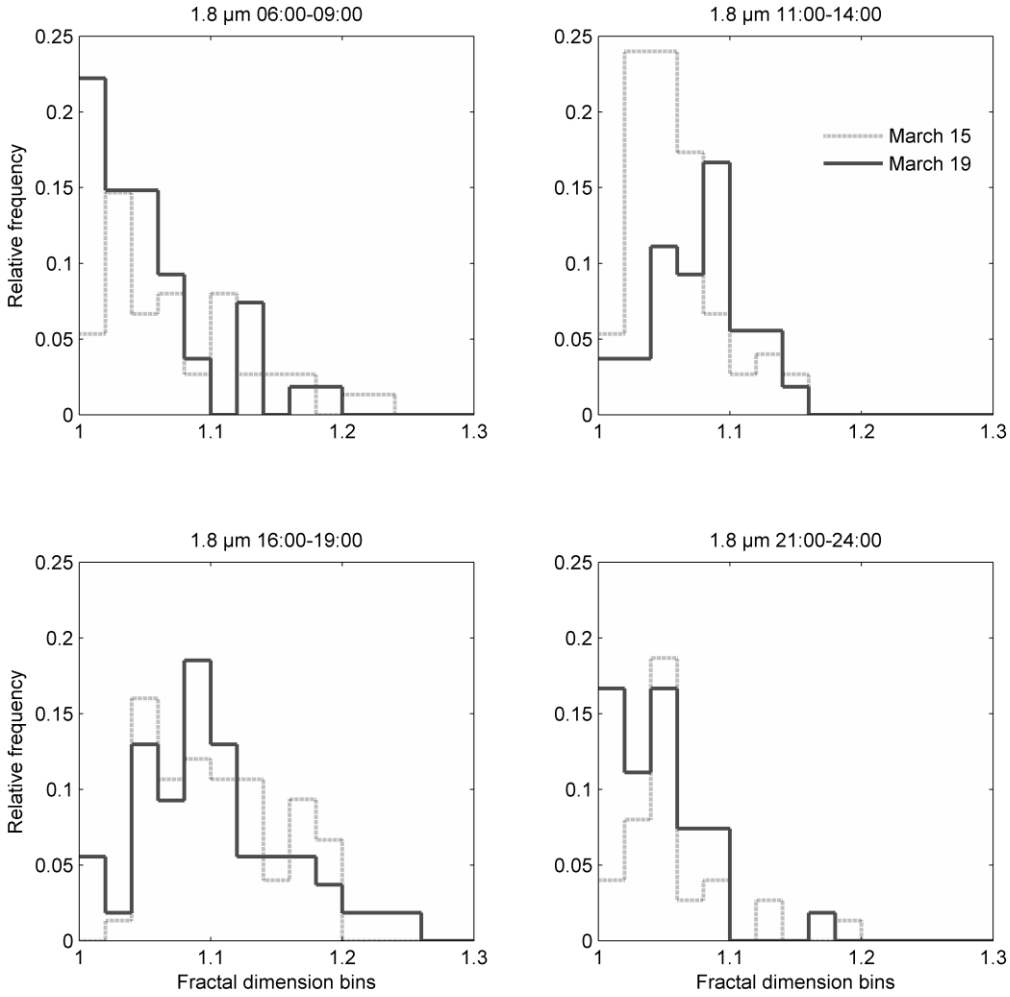

Figure 6 D_f particles histograms (1.8 µm aerodynamic diameter), sorted by sampling time.

Table 1 Absorption and scattering coefficients from three different sites

Coefficient	T1	Pico de Orizaba	Mexico City (T0)
σ_{abs} (Mm^{-1})	28	17	37
σ_{sct} (Mm^{-1})	53	39	105

Table 2 Fractal dimension statistics for atmospheric particles analyzed on TEM

Aerodynamic diameter = 0.18 µm								
	March 15				March 19			
	06:00	11:00	16:00	21:00	06:00	11:00	16:00	21:00
Number	36	32	56	51	54	44	37	50
Minimum	1.03	1.01	1.01	1.03	1.01	1.02	1.01	1.02
Maximum	1.31	1.21	1.25	1.25	1.31	1.26	1.25	1.27
Average	1.15	1.09	1.07	1.09	1.10	1.08	1.08	1.11
Standard dev	0.08	0.06	0.04	0.05	0.06	0.06	0.06	0.07

Table 3 Fractal dimension statistics for atmospheric particles analyzed on TEM

Aerodynamic diameter = 1.8 µm								
	March 15				March 19			
	06:00	11:00	16:00	21:00	06:00	11:00	16:00	21:00
Number	42	65	61	31	41	32	47	33
Minimum	1.01	1.01	1.03	1.00	1.00	1.01	1.01	1.00
Maximum	1.23	1.16	1.19	1.18	1.20	1.32	1.24	1.18
Average	1.08	1.06	1.10	1.05	1.05	1.08	1.10	1.05
Standard dev	0.06	0.03	0.05	0.04	0.05	0.05	0.06	0.04

Table 4 Elemental composition of atmospheric particles (1.8 and 0.18 µm aerodynamic diameters) sampled on March 15 and 19. Average results for particles analyzed on Figure 3, weight percent.

Element	March 15		March 19	
	1.8 µm	0.18 µm	1.8 µm	0.18 µm
C	5.8	21.7	3.9	77.9
O	15.7	4.6	18.4	11.1
Na	4.7		67.7	
Mg	2.2		3.5	
Al	5.3			
Si	19	6.1	0.3	9
P	0.9			
S	3.9		4.0	
K	1		0.6	1.1
Ca	38		0.6	
Fe	3.4	33.3		
Co		34.3		